Thiolated Gold Nanowires: Metallic *versus* Semiconducting

De-en Jiang,[†,*] Katsuyuki Nobusada,[‡] Weidong Luo,[§,∥] and Robert L. Whetten[¶]

[†]Chemical Sciences Division, Oak Ridge National Laboratory, Oak Ridge, Tennessee 37831, [‡]Department of Theoretical and Computational Molecular Science, Institute for Molecular Science, Myodaiji, Okazaki 444-8585, Japan, [§]Department of Physics and Astronomy, Vanderbilt University, Nashville, Tennessee 37235, [∥]Materials Science and Technology Division, Oak Ridge National Laboratory, Oak Ridge, Tennessee 37831, and [¶]School of Chemistry & Biochemistry, Georgia Institute of Technology, Atlanta, Georgia 30332

ABSTRACT Tremendous research efforts have been spent on thiolated gold nanoparticles and self-assembled monolayers of thiolate (RS—) on gold, but thiolated gold nanowires have received almost no attention. Here we computationally design two such one-dimensional nanosystems by creating a linear chain of Au icosahedra, fused together by either vertex sharing or face sharing. Then neighboring Au icosahedra are bridged by five thiolate groups for the vertex-sharing model and three RS—Au—SR motifs for the face-sharing model. We show that the vertex-sharing thiolated gold nanowire can be made either semiconducting or metallic by tuning the charge, while the face-sharing one is always metallic. We explain this difference between the two nanowires by examining their band structures and invoking a previously proposed electron-count rule. Implications of our findings for previous experimentation of gold nanowires are discussed, and a potential way to make thiolated gold nanowires is proposed.

KEYWORDS: gold nanowires · thiolate · semiconducting · density functional theory · band structure

The favorable interaction between thiolate and gold manifests in two famous examples: self-assembled monolayers (SAMs) of thiolate on gold[1] and thiolate-protected gold (Au:SR) nanoparticles.[2−4] The former typifies a two-dimensional system, while the latter zero-dimensional. Both systems have enjoyed tremendous attention since their discoveries in 1980s and 1990s, respectively.

Research of SAMs and Au:SR nanoparticles has advanced greatly in the past several years. In the area of SAMs, the observation of RS−Au−SR motifs on Au(111) by low-temperature scanning tunneling microscopy[5] called for a re-interpretation of previous experimental data.[6,7] The total-structure determination of $Au_{102}(SR)_{44}$ (**1**)[8,9] and $Au_{25}(SR)_{18}^-$ (**2**)[10,11] demonstrated the structural characteristics of stable Au:SR clusters: a high-symmetry Au core protected by the linear RS−Au−SR (short) and the V-shaped RS−Au−SR−Au−SR (long) motifs. The short motif is a common structural feature shared by both the SAMs on Au and Au:SR nanoparticles. Recently, the long motif has also been computationally explored on Au(111).[12] Moreover, the superatom concept has been successfully applied to explain the exceptional stability of **1** and **2**.[13,14]

Despite the tremendous research efforts on SAMs and Au:SR nanoparticles, there has been no report, experimental or computational, on the thiolated gold one-dimensional nanosystems. One-dimensional metallic nanowires often display unique electron-transport properties that can be exploited for sensing.[15] Introducing organic ligands on the nanowire surface provides a means to further tune the properties of the one-dimensional nanosystem. In this paper, we seek to computationally explore thiolated Au nanowires, by capitalizing on the recent advances in understanding the Au−thiolate interface and the electronic structure of the ligand-protected Au nanoclusters. We show that a thiolated gold nanowire can be made semiconducting, even though gold itself is an excellent conductor.

RESULTS

We envision a gold nanowire formed by a linear chain of vertex- or face-sharing icosahedra, which is then ligated on the outside by thiolate groups (in this paper, methylthiolate is chosen for convenience). This idea is reminiscent of Teo and coworkers' idea of clusters of clusters[16−18] that transition-metal icosahedral clusters assemble into bigger clusters by vertex sharing. Our model of the vertex-sharing thiolated gold nanowire is also motivated by the fact that a vertex-sharing biicosahedral gold cluster has been synthesized.[19] In this cluster, five thiolate groups are found to bridge two icosahedra. On the other hand, the face-sharing model is motivated by

*Address correspondence to jiangd@ornl.gov.

Received for review May 14, 2009 and accepted July 03, 2009.

Published online July 15, 2009.
10.1021/nn900498c CCC: $40.75

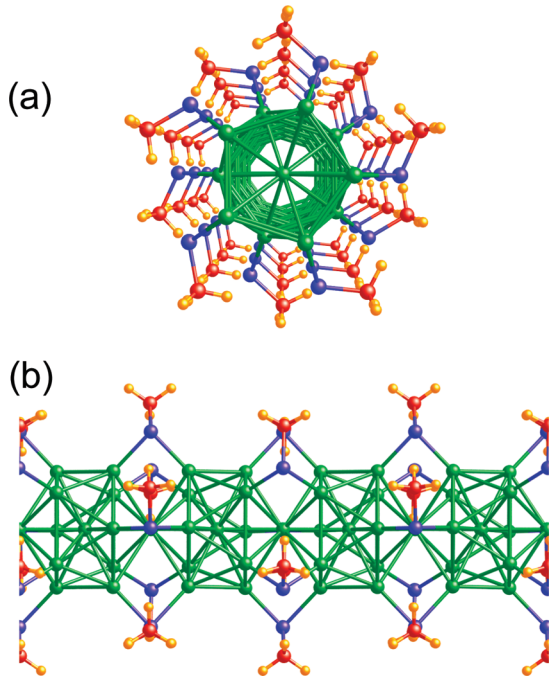

Figure 1. Vertex-sharing icosahedral thiolated gold nanowire: (a) viewed along the wire; (b) side view. Au, green; S, blue; C, red; H, orange.

the proposed face-sharing biicosahedral structure for $Au_{38}(SR)_{24}$,[20] which has been shown to be more stable than all previous models.[21−24] In this biicosahedral structure, three RS−Au−SR motifs are found to bridge two icosahedra.

From the previous work on biicosahedral Au clusters described above, it is natural for us to create a vertex-sharing icosahedral gold nanowire bridged by five thiolate groups and a face-sharing one bridged by three RS−Au−SR motifs. We examine the geometry, band structure, and density of states first of the vertex-sharing thiolated gold nanowire and then of the face-sharing one. For comparison, we also study the bare Au wires without the thiolate or RS−Au−SR ligands.

Looking along the vertex-sharing thiolated gold nanowire (Figure 1a), one can see that the wire has a C_5 symmetry. The side view (Figure 1b) displays two unit cells of the wire, each of which consists of two vertex-sharing icosahedra with a formula of $Au_{24}(SR)_{10}$. The biicosahedral $Au_{24}S_{10}$ framework in the unit cell has a point group of D_{5h} approximately, and the two neighboring Au icosahedra are bridged together by five thiolate groups.

We optimized the repeating length for the wire for different charge states of the unit cell and found that the neutral and +2 states have a similar optimal length of 11.3 Å, while the −2 state has 11.5 Å. We plot the neutral state's band structure near the Fermi level in Figure 2. The Fermi level crosses both bands 5 and 6, so the neutral wire is metallic, and analysis of the two bands shows that they are dominated by the Au states (for example, see Figure 3 for band 5). Interestingly, we found that a gap separates bands 6 and 7 and another gap separates degenerate bands (3,4) and band 5, indicating that both the −2 and +2 states are semiconducting. We confirmed that this is indeed the case by examining the band structures for both charge states at their respective optimal repeating length. The band structure in Figure 2 also shows an interesting feature that bands (5,6) have a degenerate point at $k = \pi/a$. This is also the case for bands (1,2), (3,4), and (7,8). What this implies is that each pair of bands originates from a single band that folds back into the Brillouin zone because of doubling the unit cell. This explanation agrees well with the fact that the unit cell of the wire contains two icosahedra, and there is perfect inversion symmetry at the center of each icosahedron and perfect mirror symmetry between adjacent icosahedra. So the single-band origin can be viewed as resulting from a single icosahedron repeating unit.

The total density of states (DOS) of the vertex-sharing wire (Figure 4) again confirms that the neutral state is metallic, and there is a gap around −0.3 and 0.5 eV that corresponds to the +2 and −2 states, respectively. On the contrary, the bare vertex-sharing Au wire at the same repeating length is metallic for a wide range of energy around the Fermi level (Figure 5). This contrast clearly illustrates how ligands affect the electronic structure of the gold nanowire, a basis for utilizing gold nanowires for sensing.

We now turn to the facing-sharing icosahedral thiolated Au wire (Figure 6). This structure is derived from the proposed face-sharing biicosahedral structure for $Au_{38}(SR)_{24}$ whose two neighboring icosahedra are bridged by three RS−Au−SR motifs.[20] The face-sharing nanowire has a C_3 symmetry along the repeating axis (Figure 6a), and the side view (Figure 6b) displays two repeating unit cells. Each unit cell has a formula of $Au_{26}(SR)_{12}$. Compared with the vertex-sharing thiolated Au wire, the face-sharing wire is more closely packed in

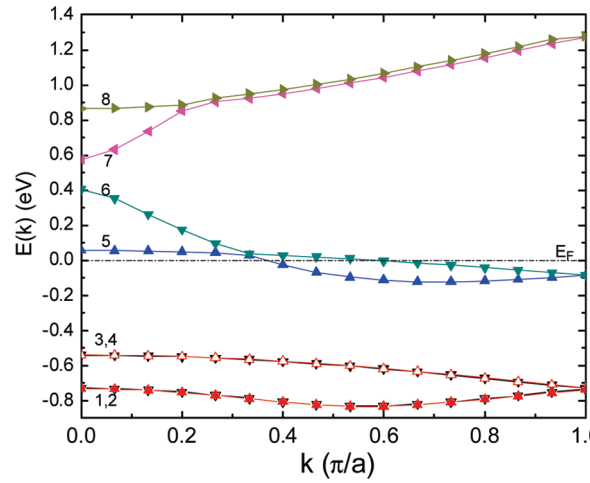

Figure 2. Band structure of the vertex-sharing icosahedral thiolated gold nanowire.

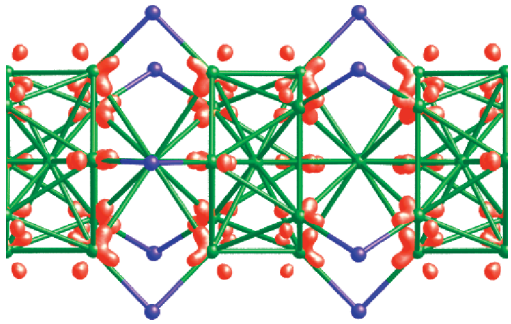

Figure 3. Electron density isosurface (in red) of band 5 of the vertex-sharing thiolated gold nanowire. Isovalue at 0.02 e/Å^3. Au, green; S, blue; C and H, not shown.

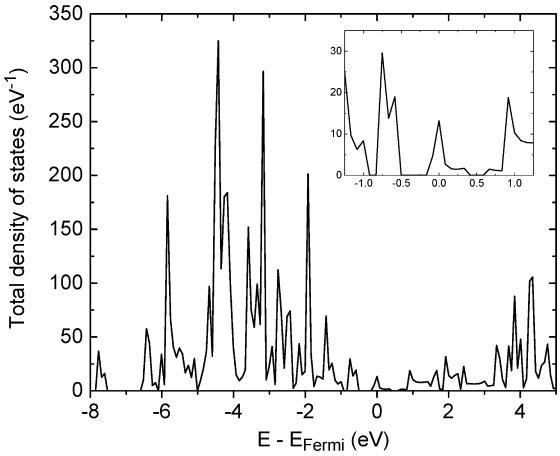

Figure 4. Total electronic density of states of the vertex-sharing icosahedral thiolated gold nanowire. The inset is zoom-in of −1.25 to 1.25 eV.

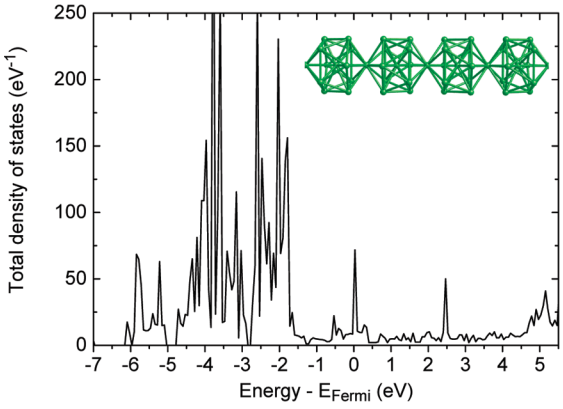

Figure 5. Total electronic density of states of the bare vertex-sharing icosahedral gold nanowire.

the center, as evidenced by the smaller optimal repeating length (at 8.74 Å for the neutral state) and greater one-dimensional density (2.3 *versus* 2.1 Au/Å for the vertex-sharing structure). This closer packing also results in stronger interaction among Au atoms along the chain, leading to greater dispersion of bands near the Fermi level (Figure 7). One can see that bands 3, 4, and 5 show relatively greater dispersion. Analysis of band 3 shows that it is also dominated by the Au states (Figure 8). As a result, this face-sharing Au:SR wire is metallic

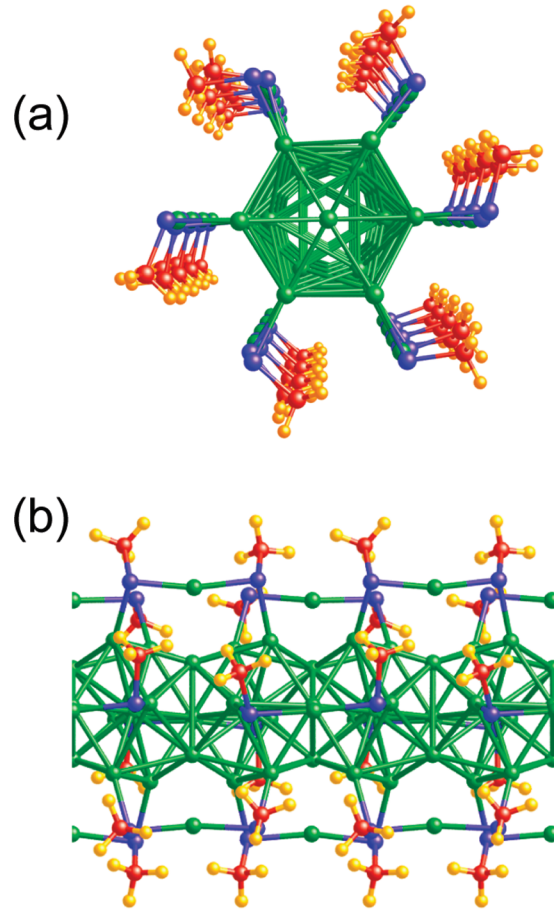

Figure 6. Face-sharing icosahedral thiolated gold nanowire: (a) viewed along the wire; (b) side view. Au, green; S, blue; C, red; H, orange.

for a wide range of energy around the Fermi level (Figure 9), though the DOS varies greatly with energy around the Fermi level, which has to do with the band structure in that energy range (Figure 7).

For comparison, in Figure 10, we plot the DOS of the bare face-sharing Au wire at the same repeating length but without the RS−Au−SR ligands. One can see that this wire is metallic across the energy range shown in Figure 10. Unlike the thiolated Au wire, the bare Au wire shows less variation in DOS around the

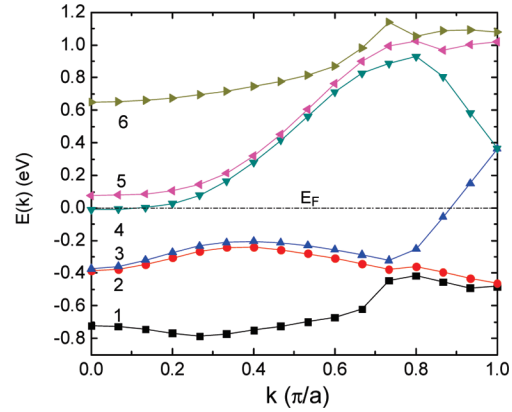

Figure 7. Band structure of the face-sharing icosahedral thiolated gold nanowire.

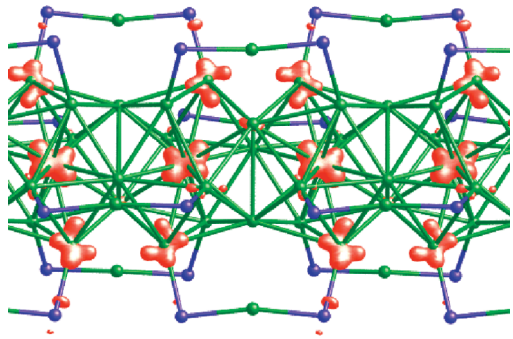

Figure 8. Electron density isosurface (in red) of band 3 of the face-sharing thiolated gold nanowire. Isovalue at 0.02 e/Å^3. Au, green; S, blue; C and H, not shown.

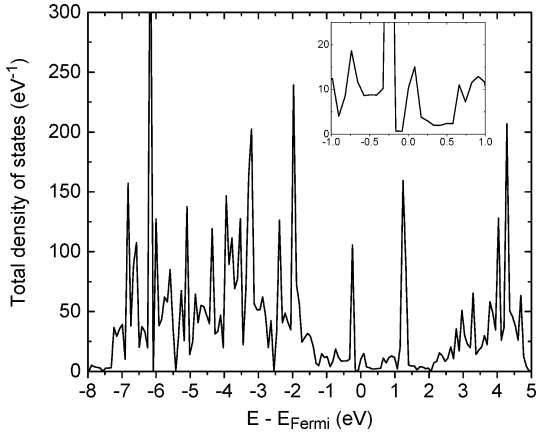

Figure 9. Total electronic density of states of the face-sharing icosahedral thiolated gold nanowire. The inset is zoom-in of −1.0 to 1.0 eV.

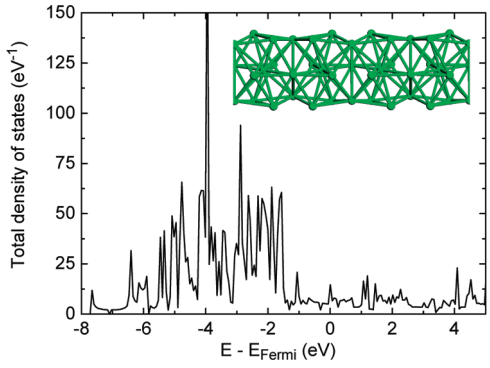

Figure 10. Total electronic density of states of the bare face-sharing icosahedral gold nanowire.

Fermi level, indicating greater contribution of gold 6s electrons to the DOS at the Fermi level for the bare wire. After complexation by RS−Au−SR ligands, some 6s electrons from the center wire are localized, leading to narrower dispersion of some bands (for example, band 2 and a large part of band 3 in Figure 7) and therefore sharp peaks in the DOS around the Fermi level (for example, the peak at −0.25 eV in Figure 9).

For both the vertex-sharing and face-sharing thiolated gold nanowires examined here, we have assumed a symmetric configuration for the methylthiolate groups which all adopt the same conformation. In reality, the methyl group can choose to be on either side of the plane determined by the Au−S−Au bond. We considered the scenario where one methyl group is flipped to the other side for both the vertex-sharing and face-sharing thiolated gold nanowires. We found that the flipping changed the energetics, geometry, and electronic structure only slightly and that the qualitative nature of the wire (such as the existence of the semiconducting states for the vertex-sharing wire) was not affected.

DISCUSSION

The thiolated gold nanowires examined above both have their cluster (or oligomer) counterparts. As for clusters, there are rules of electron count that explain their stability. How can one relate these electron-count rules to the one-dimensional wires? How do these electron-count rules explain the semiconducting and metallic behaviors we have found for the two nanowires? Moreover, how can we relate our findings here to previous experiments such as gold nanowires for sensing? We discuss these questions below.

A cluster with the icosahedral structure is quite rigid and therefore can serve as a building block for assemblies of the clusters into polyicosahedra. Teo and co-workers[16−18] have pioneered this idea by synthesizing many mixed-metal vertex-sharing polyicosahedra nanoclusters. The recently discovered $[Au_{25}(PPh_3)_{10}(SC_2H_5)_5Cl_2]^{2+}$ cluster belongs to this category of vertex-sharing polyicosahedra.[19] This cluster has a biicosahedral structure where five thiolate groups bridge the two icosahedra. Extending this structure to a linear trimer, Nobusada and Iwasa[25] studied the electronic structures of both the biicosahedral and triicosahedral clusters with the DFT/B3LYP method. They concluded that Mingos's electron-count rule[26] for vertex-sharing clusters applies to the dimer and trimer clusters.

Here we give a brief summary of Mingos's electron-count rule. Mingos and co-workers[26] concluded that the vertex-sharing icosahedra of clusters of group 11 elements have a rather open structure, and therefore, the molecular orbitals of the condensed clusters correspond to the summation of the 1s and 1p orbitals of the electron-shell model for each icosahedron. In other words, the vertex-sharing icosahedra can be viewed as a cluster of weakly interacting superatoms each having a shell-closing electron count of 8;[13,14] hence, the total electron count is $8n_p$, where n_p is the number of icosahedra.[26] This electron-count rule can be nicely extended to our vertex-sharing thiolated Au nanowire (Figure 1), which is just a linear chain of vertex-sharing icosahedra. The unit cell of the vertex-sharing thiolated Au nanowire is a biicosahedra with a formula of $Au_{24}(SR)_{10}$, which gives an electron count of 12, 14, and 16 per unit cell (or per biicosahedra) for the +2, neutral, and −2 charge states, respectively.[27] The electron count 16

corresponds to the shell closing of two icosahedra, and that is why the −2 charge state has a band gap and is semiconducting. The electron count 14 corresponds to 7 electrons per icosahedron, leading to a singly occupied $1p_z$ orbital (the symmetry breaking causes the degenerate $1p_x$ and $1p_y$ orbitals of the single icosahedron superatom to become lower in energy than $1p_z$[26]). When this $1p_z$ orbital (which is parallel to the wire) forms a band, it is half-filled, leading to a metallic state for the neutral state. The electron count 12 per unit cell (or 6 per icosahedron) corresponds to the shell closing of 1s and $1p_{x,y}$ for each icosahedron [that is, $(1s)^2(1p_{x,y})^4$], so the +2 charge state also has a band gap.

The electronic structure of the vertex-sharing wire shows that one can switch the wire's property between metallic and semiconducting by tuning the charge. Experimentally, this can be accomplished by using chemical/electrochemical oxidation/reduction of the neutral nanowire, as experimentally demonstrated for thiolated gold nanoclusters.[28,29] The other approach is to subject the thiolated gold nanowires in an experimental setup similar to field effect transistors, where the applied gate voltage can tune the wire to be n-type or p-type doped.

The face-sharing thiolated Au nanowire originates from the proposed biicosahedral structure for $Au_{38}(SR)_{24}$.[20] In their paper,[26] Mingos and co-workers also analyzed orbital interactions in a face-sharing biicosahedra. They concluded that the close packing in the face-sharing mode does not allow additive treatment of each icosahedron. Extending the face-sharing biicosahedra to a linear chain, one finds strong dispersion of bands near the Fermi level, resulting from strong orbital interactions. As a result, the face-sharing wire is metallic for a wide range of energy around the Fermi level, and no simple electron-count rule seems to apply here.

Our present computational findings can be related to experimental work in using gold nanowires for sensing applications and preparing ultrathin gold nanowires. Tao and co-workers have demonstrated that the conductance of atomically thin gold nanowires can be modulated by adsorption of molecules and solvent anions.[15,30,31] This is in agreement with our findings that the electronic structure of the gold nanowire changes greatly when it is complexed by thiolate or RS−Au−SR ligands. A more direct comparison with experiment here would require computing electronic conductance through the thiolated gold nanowires, which is planned for the future. Moreover, Tao and co-workers found that the Au quantum wires elongate after adsorption of molecules.[15] This observation also agrees with our findings. For example, we found that the optimal repeating length for the bare vertex-sharing icosahedral wire is 10.5 Å, while that for the corresponding thiolated Au wire is elongated to 11.3 Å. Furthermore, Kondo and Takayanagi[32] have synthesized helical multishell gold nanowires in an ultrahigh vacuum. The thinnest wire they made was 0.6 nm in diameter, corresponding to a two-shell nanowire. This thinnest wire is quite similar to the bare gold nanowires shown in our Figures 5 and 10, which also have a two-shell structure and a similar diameter. Therefore, it would be interesting to examine how adsorption of thiol molecules affects the conductance of Kondo and Takayanagi's helical gold nanowires.

Another recent experimental progress is the synthesis of sub-2 nm Au nanowires from wet chemistry.[33,34] This progress brings up an opportunity to make one-dimensional thiolated gold, as one has done for zero-dimensional thiolated gold nanoclusters or two-dimensional self-assembled monolayers of thiolate on a flat gold surface. One obvious way is to react the synthesized sub-2 nm Au nanowires with neat thiols to see if thiolate groups can self-assemble on the nanowire. Here it would be desirable to know the relative stability of the two thiolated gold nanowires examined, so we could offer experimentalists a guide in terms of what to expect when reacting gold nanowires with thiols. Because the two thiolated gold nanowires have different Au/SR ratios, we cannot compare their relative stability directly, but we can use the following reaction to relate the two wires against a known compound $[Au_4(SR)_4]$:[35]

$$Au_{24}(SR)_{10} + 1/2\ Au_4(SR)_4 \rightarrow Au_{26}(SR)_{12}$$

where $Au_{24}(SR)_{10}$ and $Au_{26}(SR)_{12}$ are the unit cell formula for the vertex-sharing and face-sharing wires, respectively. We found that this reaction is downhill by 0.41 eV. In other words, in the presence of $Au_4(SR)_4$, the vertex-sharing wire is not stable against the formation of the face-sharing wire. This result is consistent with what we and others have found on gold particle surfaces and on the flat Au(111) surface; namely, the RS−Au−SR motif is preferred over the isolated adsorption of the thiolate group.[6,24]

CONCLUSIONS

Using density functional theory with the generalized gradient approximation for electron exchange and correlation, we have studied thiolated Au nanowires in two configurations: a vertex-sharing icosahedral chain bridged by five thiolate groups and a face-sharing icosahedral chain bridged by three RS−Au−SR ligands. We found that the vertex-sharing thiolated gold nanowire is metallic for the neutral state but semiconducting for the −2 and +2 charge states on the basis of the biicosahedral unit cell. This electronic structure can be understood by applying the electron-count rule introduced by Mingos and co-workers;[26] namely, the vertex-sharing thiolated gold nanowires can be viewed as a chain of weakly inter-

acting individual icosahedra. Each icosahedron is a superatom where electron counts of 6 and 8 (corresponding to the +2 and −2 states for the biicosahedral unit cell, respectively) lead to closed shells (therefore, semiconducting states for the chain), while the electron count of 7 (corresponding to the neutral state) gives rise to a singly occupied orbital (therefore, metallic state for the chain). We found that the face-sharing thiolated gold is always metallic. This is due to the more closely packed structure of the face-sharing mode which results in greater interaction among icosahedra and hence greater dispersion of bands near the Fermi level. Our findings have implications for using Au nanowires for sensing, and we have suggested a potential way to realize thiolated gold nanowires based on recent experimental progress in synthesizing sub-2 nm gold nanowires from wet chemistry.

METHODS

We used the Vienna *Ab Initio* Simulation Package (VASP)[36,37] to perform density functional theory (DFT) calculations with planewave bases and periodic boundary conditions. The Perdew−Burke−Erzonhoff (PBE) form of the generalized gradient approximation (GGA) was chosen for electron exchange and correlation.[38] The electron−core interaction was described by the projector-augmented wave (PAW) method[39,40] within the frozen-core approximation. The standard PAW potentials from the database provided with VASP were used for Au, S, C, and H, whose valence electron configurations in the potentials are $d^{10}s^1$, s^2p^4, s^2p^2, and s^1, respectively. For Au, scalar relativistic corrections were included in the PAW potential. A converged kinetic energy cutoff of 450 eV was employed. The supercell approach was employed to model the Au:SR nanowires. The wires are repeated along the *z*-axis and separated from its periodic images in the *x*- and *y*-axis by 10 Å vacuum. To model the charged unit cells, a compensating homogeneous background charge was employed.[41] Atomic positions were optimized at various fixed repeating lengths to obtain the optimal length. Force convergence criterion for geometry optimization was set at 0.05 eV/Å; 32 *k*-points were used to sample the one-dimensional Brillouin zone.

Acknowledgment. This work was supported by Office of Basic Energy Sciences, U.S. Department of Energy under Contract No. DE-AC05-00OR22725 with UT-Battelle, LLC. D.E.J. acknowledges useful discussions with X.Q. Chen and V. Meunier. This research used resources of the National Energy Research Scientific Computing Center, which is supported by the Office of Science of the U.S. Department of Energy under Contract No. DE-AC02-05CH11231. K.N. acknowledges the financial support of Grant-in-Aid (No. 18066019) from the Ministry of Education, Culture, Sports, Science and Technology of Japan.

REFERENCES AND NOTES

1. Love, J. C.; Estroff, L. A.; Kriebel, J. K.; Nuzzo, R. G.; Whitesides, G. M. Self-Assembled Monolayers of Thiolates on Metals as a Form of Nanotechnology. *Chem. Rev.* **2005**, *105*, 1103.
2. Brust, M.; Walker, M.; Bethell, D.; Schiffrin, D. J.; Whyman, R. Synthesis of Thiol-Derivatized Gold Nanoparticles in a 2-Phase Liquid-Liquid System. *J. Chem. Soc., Chem. Commun.* **1994**, 801.
3. Whetten, R. L.; Khoury, J. T.; Alvarez, M. M.; Murthy, S.; Vezmar, I.; Wang, Z. L.; Stephens, P. W.; Cleveland, C. L.; Luedtke, W. D.; Landman, U. Nanocrystal Gold Molecules. *Adv. Mater.* **1996**, *8*, 428.
4. Templeton, A. C.; Wuelfing, M. P.; Murray, R. W. Monolayer Protected Cluster Molecules. *Acc. Chem. Res.* **2000**, *33*, 27.
5. Maksymovych, P.; Sorescu, D. C.; Yates, J. T. Gold-Adatom-Mediated Bonding in Self-Assembled Short-Chain Alkanethiolate Species on the Au(111) Surface. *Phys. Rev. Lett.* **2006**, *97*, 146103.
6. Grönbeck, H.; Häkkinen, H.; Whetten, R. L. Gold−Thiolate Complexes Form a Unique $c(4 \times 2)$ Structure on Au(111). *J. Phys. Chem. C* **2008**, *112*, 15940.
7. Cossaro, A.; Mazzarello, R.; Rousseau, R.; Casalis, L.; Verdini, A.; Kohlmeyer, A.; Floreano, L.; Scandolo, S.; Morgante, A.; Klein, M. L.; Scoles, G. X-ray Diffraction and Computation Yield the Structure of Alkanethiols on Gold(111). *Science* **2008**, *321*, 943.
8. Jadzinsky, P. D.; Calero, G.; Ackerson, C. J.; Bushnell, D. A.; Kornberg, R. D. Structure of a Thiol Monolayer-Protected Gold Nanoparticle at 1.1 Angstrom Resolution. *Science* **2007**, *318*, 430.
9. Whetten, R. L.; Price, R. C. Nano-Golden Order. *Science* **2007**, *318*, 407.
10. Heaven, M. W.; Dass, A.; White, P. S.; Holt, K. M.; Murray, R. W. Crystal Structure of the Gold Nanoparticle $[N(C_8H_{17})_4][Au_{25}(SCH_2CH_2Ph)_{18}]$. *J. Am. Chem. Soc.* **2008**, *130*, 3754.
11. Zhu, M.; Aikens, C. M.; Hollander, F. J.; Schatz, G. C.; Jin, R. Correlating the Crystal Structure of a Thiol-Protected Au_{25} Cluster and Optical Properties. *J. Am. Chem. Soc.* **2008**, *130*, 5883.
12. Jiang, D. E.; Dai, S. Constructing Gold−Thiolate Oligomers and Polymers on Au(111) Based on the Linear S−Au−S Geometry. *J. Phys. Chem. C* **2009**, *113*, 7838.
13. Walter, M.; Akola, J.; Lopez-Acevedo, O.; Jadzinsky, P. D.; Calero, G.; Ackerson, C. J.; Whetten, R. L.; Gönbeck, H.; Häkkinen, H. A. Unified View of Ligand-Protected Gold Clusters as Superatom Complexes. *Proc. Natl. Acad. Sci. U.S.A.* **2008**, *105*, 9157.
14. Akola, J.; Walter, M.; Whetten, R. L.; Häkkinen, H.; Grönbeck, H. On the Structure of Thiolate-Protected Au_{25}. *J. Am. Chem. Soc.* **2008**, *130*, 3756.
15. He, H. X.; Tao, N. J. Interactions of Molecules with Metallic Quantum Wires. *Adv. Mater.* **2002**, *14*, 161.
16. Teo, B. K.; Shi, X. B.; Zhang, H. Cluster of Clusters. Structure of a Novel Cluster $[(Ph_3P)_{10}Au_{13}Ag_{12}Br_8](SBF_6)$ Containing an Exact Staggered Eclipsed Staggered Metal Configuration. Evidence of Icosahedral Units as Building Blocks. *J. Am. Chem. Soc.* **1991**, *113*, 4329.
17. Teo, B. K.; Zhang, H. Clusters of Clusters: Self-Organization and Self-Similarity in the Intermediate Stages of Cluster Growth of Au−Ag Supraclusters. *Proc. Natl. Acad. Sci. U.S.A.* **1991**, *88*, 5067.
18. Teo, B. K.; Zhang, H. Polyicosahedricity: Iicosahedron to Icosahedron of Icosahedra Growth Pathway for Bimetallic (Au−Ag) and Trimetallic (Au−Ag−M, M = Pt, Pd, Ni) Supraclusters. Synthetic Strategies, Site Preference, and Stereochemical Principles. *Coord. Chem. Rev.* **1995**, *143*, 611.
19. Shichibu, Y.; Negishi, Y.; Watanabe, T.; Chaki, N. K.; Kawaguchi, H.; Tsukuda, T. Biicosahedral Gold Clusters $[Au_{25}(PPh_3)_{10}(SC_2H_5)_5Cl_2]^{2+}$ ($n = 2-18$): A Stepping Stone to Cluster-Assembled Materials. *J. Phys. Chem. C* **2007**, *111*, 7845.
20. Pei, Y.; Gao, Y.; Zeng, X. C. Structural Prediction of Thiolate-Protected Au_{38}: A Face-Fused Bi-Icosahedral Au Core. *J. Am. Chem. Soc.* **2008**, *130*, 7830.
21. Garzon, I. L.; Rovira, C.; Michaelian, K.; Beltran, M. R.; Ordejon, P.; Junquera, J.; Sanchez-Portal, D.; Artacho, E.; Soler, J. M. Do Thiols Merely Passivate Gold Nanoclusters? *Phys. Rev. Lett.* **2000**, *85*, 5250.
22. Häkkinen, H.; Walter, M.; Grönbeck, H. Divide and Protect: Capping Gold Nanoclusters with Molecular Gold−Thiolate Rings. *J. Phys. Chem. B* **2006**, *110*, 9927.

23. Jiang, D. E.; Luo, W.; Tiago, M. L.; Dai, S. In Search of a Structural Model for a Thiolate-Protected Au_{38} Cluster. *J. Phys. Chem. C* **2008**, *112*, 13905.
24. Jiang, D. E.; Tiago, M. L.; Luo, W. D.; Dai, S. The "Staple" Motif: A Key to Stability of Thiolate-Protected Gold Nanoclusters. *J. Am. Chem. Soc.* **2008**, *130*, 2777.
25. Nobusada, K.; Iwasa, T. Oligomeric Gold Clusters with Vertex-Sharing Bi- and Triicosahedral Structures. *J. Phys. Chem. C* **2007**, *111*, 14279.
26. Lin, Z. Y.; Kanters, R. P. F.; Mingos, D. M. P. Closed-Shell Electronic Requirements for Condensed Clusters of the Group-11 Elements. *Inorg. Chem.* **1991**, *30*, 91.
27. For an arbitrary thiolated Au cluster, $Au_x(SR)_L^q$ (where q is the charge of the cluster), the electron count is $n = x-L-q$ (ref 13).
28. Zhu, M.; Aikens, C. M.; Hendrich, M. P.; Gupta, R.; Qian, H.; Schatz, G. C.; Jin, R. Reversible Switching of Magnetism in Thiolate-Protected Au_{25} Superatoms. *J. Am. Chem. Soc.* **2009**, *131*, 2490.
29. Chen, S. W.; Ingram, R. S.; Hostetler, M. J.; Pietron, J. J.; Murray, R. W.; Schaaff, T. G.; Khoury, J. T.; Alvarez, M. M.; Whetten, R. L. Gold Nanoelectrodes of Varied Size: Transition to Molecule-like Charging. *Science* **1998**, *280*, 2098.
30. Li, C. Z.; He, H. X.; Bogozi, A.; Bunch, J. S.; Tao, N. J. Molecular Detection Based on Conductance Quantization of Nanowires. *Appl. Phys. Lett.* **2000**, *76*, 1333.
31. Bogozi, A.; Lam, O.; He, H. X.; Li, C. Z.; Tao, N. J.; Nagahara, L. A.; Amlani, I.; Tsui, R. Molecular Adsorption onto Metallic Quantum Wires. *J. Am. Chem. Soc.* **2001**, *123*, 4585.
32. Kondo, Y.; Takayanagi, K. Synthesis and Characterization of Helical Multi-Shell Gold Nanowires. *Science* **2000**, *289*, 606.
33. Huo, Z. Y.; Tsung, C. K.; Huang, W. Y.; Zhang, X. F.; Yang, P. D. Sub-Two Nanometer Single Crystal Au Nanowires. *Nano Lett.* **2008**, *8*, 2041.
34. Lu, X. M.; Yavuz, M. S.; Tuan, H. Y.; Korgel, B. A.; Xia, Y. N. Ultrathin Gold Nanowires Can Be Obtained by Reducing Polymeric Strands of Oleylamine−AuCl Complexes Formed *via* Aurophilic Interaction. *J. Am. Chem. Soc.* **2008**, *130*, 8900.
35. Bonasia, P. J.; Gindelberger, D. E.; Arnold, J. Synthesis and Characterization of Gold(I) Thiolates, Selenolates, and Tellurolates: X-ray Crystal-Structures of $Au_4[Tec(SiMe_3)_3]_4$, $Au_4[Sc(SiMe_3)_3]_4$, and $Ph_3PAu[TeC(SiMe_3)_3]$. *Inorg. Chem.* **1993**, *32*, 5126.
36. Kresse, G.; Furthmüller, J. Efficient Iterative Schemes for *Ab Initio* Total-Energy Calculations Using A Plane-Wave Basis Set. *Phys. Rev. B* **1996**, *54*, 11169.
37. Kresse, G.; Furthmüller, J. Efficiency of *Ab Initio* Total Energy Calculations for Metals and Semiconductors Using a Plane-Wave Basis Set. *Comput. Mater. Sci.* **1996**, *6*, 15.
38. Perdew, J. P.; Burke, K.; Ernzerhof, M. Generalized Gradient Approximation Made Simple. *Phys. Rev. Lett.* **1996**, *77*, 3865.
39. Blöchl, P. E. Projector Augmented-Wave Method. *Phys. Rev. B* **1994**, *50*, 17953.
40. Kresse, G.; Joubert, D. From Ultrasoft Pseudopotentials to the Projector Augmented-Wave Method. *Phys. Rev. B* **1999**, *59*, 1758.
41. Makov, G.; Payne, M. C. Periodic Boundary-Conditions in *Ab Initio* Calculations. *Phys. Rev. B* **1995**, *51*, 4014.